Article

Strategically designing a pumpless microfluidic device on an "inert" polypropylene substrate with potential application in biosensing and diagnostics

Elham Shirani, Amir Razmjou, Hossein Tavassoli, Amir Landarani-Isfahani, Saghar Rezaei, Abolghasem Abbasi Kajani, Mohsen Asadnia, Jingwei Hou, and Majid Ebrahimi Warkiani

Langmuir, **Just Accepted Manuscript** • Publication Date (Web): 10 May 2017

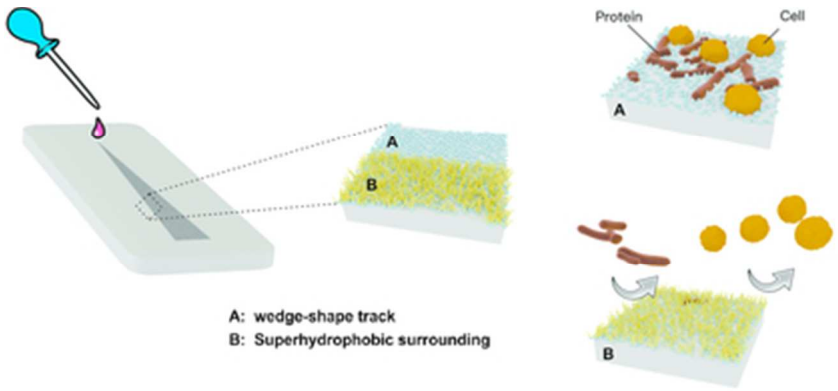

Graphical abstract

35x16mm (300 x 300 DPI)

Strategically designing a pumpless microfluidic device on an "inert" polypropylene substrate with potential application in biosensing and diagnostics

Elham Shirani[1], Amir Razmjou[1*], Hossein Tavassoli[2], Amir Landarani-Isfahani[3], Saghar Rezaei[3], Abolghasem Abbasi Kajani[1], Mohsen Asadnia[4], Jingwei Hou[5], Majid Ebrahimi Warkiani[2]

[1] Department of Biotechnology, Faculty of Advanced Sciences and Technologies, University of Isfahan, Isfahan, Iran

[2] School of Mechanical and Manufacturing Engineering, Australian Centre for NanoMedicine, University of New South Wales, Sydney, NSW 2052, Australia

[3] Department of Chemistry, University of Isfahan, Isfahan 81746-73441, Iran

[4] Department of Engineering, Macquarie University, NSW 2109, Australia

[5] UNESCO Centre for Membrane Science and Technology, School of Chemical Science and Engineering, The University of New South Wales, Sydney, 2052, Australia

Abstract

This study is an attempt to make a step forward to implement the very immature concept of pumpless transportation of liquid into a real miniaturized device or lab-on-chip (LOC) on a plastic substrate. "Inert" plastic materials such as polypropylene (PP) are used in a variety of biomedical applications but their surface engineering is very challenging. Here, it was demonstrated that with a facile innovative wettability patterning route using fluorosilanized UV-independent TiO_2 nanoparticle coating it is possible to create wedge-shape open microfluidic tracks on inert solid surfaces for low-cost biomedical devices (Lab-on-plastic). For the future miniaturization and integration of the tracks into a device, a variety of characterization techniques were used to not only systematically study the surface patterning chemistry and topography but also to have a clear knowledge of its biological interactions and performance. The effect of such surface architecture on the biological performance was studied in terms of

static/dynamic protein (bovine serum albumin) adsorption, bacterial (*staphylococcus aureus* and *staphylococcus epidermidis*) adhesion, cell viability (using HeLa and MCF-7 cancer cell lines as well as non-cancerous human fibroblast cells), and cell patterning (Murine embryonic fibroblasts). Strategies for incorporating such a confined track into a diagnostic device which its sensing portion is based on protein, microorganism, or cells are discussed. Finally, for the proof-of-principle of biosensing application, the well-known high-affinity molecular couple of BSA-antiBSA as a biological model was employed.

Keywords:

Microfluidics; wettability patterning; superhydrophobicity; biosensor; cellular patterning

1 Introduction

The concept of pumpless open based microfluidic systems has recently gained a significant attention in lab-on-a-chip (LOC) and point-of-care (POC) systems. This new emerging branch of open based microfluidic devices have gained popularity because of the elimination of pumps and valves, minimizing the risk of cross-contamination and bubble formation, fouling and adsorption of analytes, easy introduction of sample liquids, fast mixing velocity, and rapid chemical and biological reactions compared with the traditional closed-microfluidics systems [1]. However, they have not been commercially implemented in the areas of POC and LOC analytical devices. This is because (a) they have been mostly created on expensive model substrates, (b) in the past, the biological performances of such systems have not been investigated, (c) their fabrication process is complicated and costly making miniaturization and assembly difficult, (d) for bio-sensing applications, further bio-functionalization of bioreceptors can reduce the driving force and thus, hinder liquid pumpless transportation, and (e) they suffer from lack of accuracy and sensitivity.

Therefore, there is a continuing quest for pumpless open-based microfluidic systems which can be created on appropriate low-cost, versatile and abundant platforms for biological applications. For this purpose, proper patterning substrate selection is the first essential step of developing the low-cost open based surface-microfluidic devices. Papers and plastics (mainly polystyrene, polypropylene, and polycarbonate) are good candidates for the mass production of these devices. Recently, attempts have been made to introduce pumpless open-air "paper" based microfluidic devices to produce POC and LOC analytical devices [1e]. Although wettability patterning on papers is doable, these substrates suffer from drawbacks such as flexibility and bending ability which creates distortion and interruption during liquid transportation. Moreover, low mechanical stability (easy to tear), the difficulty of storage under the humid condition, and their porous nature which requires prefilling limits their utility in designing such a pumpless open-air microfluidic devices [2]. The aforementioned issues are not inherent to plastic materials but their "inert" nature makes the wettability patterning process a very challenging task [3]. One of the main issues in biosensors is non-specific bonding. Biological and clinical samples usually have a complex composition and matrix that can non-specifically adhere to the active, passivated, and untreated areas of the sensor surface leading to false positives and compromising the reliability of the system. Anti-fouling agents serve to prevent non-specific binding and increase the detection accuracy of target molecules. Polypropylene (PP) is known as an inert polymer with a very low tendency for bonding to biomolecules. Using PP film is attractive for biosensing as it requires no need or very low concentration of antifouling agent on its surface. In addition, it is inexpensive and fabrication of biomedical structures/devices from PP is simple and well established. Although PP has many advantages, surface modification of such PP based devices is challenging due to its inert nature.

Most of the reported approaches for wettability patterning are not cost-effective and do not lead to a permanent surface free energy gradient or Laplace pressure difference which are the main driving forces of pumpless transposition. To date, there is no systematic investigation on the biological performance of such a pumpless surface architecture in terms of static and dynamic protein adsorption, bacterial attachment, cell viability and stem cell patterning.

In this work, we propose a pumpless microfluidic device which benefits from the strength of previously reported devices while does not possess their Achilles' heel. Inexpensive polypropylene (PP) has widespread applications in biomaterials; however, so far no one has been able to utilize it in open microfluidic devices because of its "inert" nature which makes its surface modification challenging.

Firstly, we introduced a facile and cost-effective method using wet chemistry as an alternative approach to the conventional expensive plasma routs for the surface activation of inert PP films. In this method, initially, the sheet was obtained via hydrophilization of the surface by mild and efficient chemical oxidation and grafting of carboxylic groups. We previously showed that a careful low temperature hydrothermal (LTH) coating of TiO_2 nanoparticles can induce a permanent superhydrophilicity [4] or superhydrophobicity [5] without the need of any UV illumination. We also showed that these extreme wettability modifications are quite stable even at high shear flow or Reynold numbers which are far above the shears existing in the currently used POC or LOC systems. In a separate study [6] we showed that the LTH coating of TiO_2 nanoparticles is biocompatible. All of these experiences were called to create a surface free energy gradient on the low-cost inert PP films. In order to increase the driving force of the pumpless liquid transportation, a wedge-shape track was created on PP films to bring a higher Laplace pressure difference forces into play. We also considered the thermal, chemical,

mechanical, and long-term robustness of the surface modification for the stability characterization of open microfluidic devices. This is because the hydrophobic border of the hydrophilic pathway in an open microfluidic device plays an essential role in guiding the liquid stream and maintaining the device performance [7]. Such stability investigations have not been conducted in other open microfluidics studies.

What has not also been investigated in the literature is how such a spatial gradient in surface free energy can interact with biomolecules, microbes, normal and cancer cells, and stem cells. Since the pumpless microfluidic systems are going to be integrated into LOC and POC systems, the patterned hydrophilic track needs to be bio-functionalized by different bioreceptors such as enzymes, proteins, whole cells, bacteria and etc. This bio-functionalization may alter the surface chemistry and structure, which may reduce the surface free energy and wettability gradients, consequently, hinders the pumpless transportation of liquids on the chip. Therefore, it is critical to study the microfluidic systems based on its final application. Here, the biological performance of our pumpless microfluidic system was finally studied systematically.

This study demonstrates the ability to create low-cost, self-driven microfluidic devices that are able to perform liquid flow without the need of pumps, walls, and channels. Our novel cost-effective comprehensive system demonstrates the potential for further applications in testing, controlling, sampling, Lab-on-plastic reactions, and selectively manipulating small liquid volumes.

2 Experimental

2.1 Materials

Chromium (VI) oxide, acetic anhydride, acetic acid, succinic anhydride (SA), pyridine and titanium (IV) isopropoxide (TTIP) (97%) as TiO_2 precursor were purchased from Sigma–Aldrich

and used without further purification. Anhydrous ethanol, 2,4-pentanedione and perchloric acid (70%) and H, 1H, 2H, 2H-perfluor- ododecyltrichlorosilane (FTCS) powder were also supplied from Sigma. RPMI-1640 medium, dimethyl sulfoxide (DMSO), fetal calf serum (FCS), nutrient broth bacterial culture media, 3-(4,5-dimethylthiazol-2-yl)-2,5-diphenyltetrazolium bromide (MTT), and bovine serum albumin (BSA) were purchased from Sigma-Aldrich and Murine embryonic fibroblasts, C3H/10T1/2, Clone 8 (ATCC® CCL226™), Dulbecco's Modified Eagle's Medium (DMEM, high glucose, GlutaMAX™ Supplement, Gibco, Life Technologies Australia), FBS (Gibco, Life Technologies Australia), Penicillin-Streptomycin (Gibco, Life Technologies Australia), Live-Dead staining (Sigma-Aldrich, #04511-1KT-F, Castle Hill NSW, Australia) were used for biological investigations.

2.2 Method

2.2.1 Polypropylene film preparation

Polypropylene (PP) film samples were obtained by injection molding of its granules. PP films were first washed with ethanol and then were rinsed with ultrapure Milli-Q water. The samples were sonicated for 20 min and then dried for 1 h at 60°C before use.

2.2.2 Surface activation of PP films

Oxidation of PP Film (PP-O)

The oxidation of PP was performed according to the modified reported method [8]. Typically, a slice of PP (30 × 10 × 3 mm) was placed in a glass tube containing mixture of chromium (VI) oxide (300 mg, 3 mmol), acetic acid (3 mL), and acetic anhydride (3 mL) which was subsequently purged with inert atmosphere for 10 min. Next, the film sample was allowed to react at room temperature for 24 h. After the treatment, the oxidation solution was removed. The film sample was then washed with 1 M NaOH (2 × 20 mL), 1 M HC1 (2 × 20 mL), water (2 × 20 mL) methanol (3 × 20 mL), and

dichloromethane (3 × 20 mL), respectively. Finally, the oxidized PP was dried in vacuum oven at 40 °C for 4 h.

Preparation of PP-COOH

The PP-O film slice was placed in a glass tube containing a solution of succinic anhydride (SA) (100 mg) and pyridine (1 mL) in acetone (25 mL). The film sample was allowed to react at room temperature for 24 h. The solution was removed and the sample was washed with methanol (3 × 20 mL) and dichloromethane (3 × 20 mL). The PP-COOH was dried under reduced pressure at 40 °C for 4 h.

2.2.3 Wettability gradient creation

Preparation of hydrophilic PP-TiO_2 layer

The TiO_2 thin film was coated onto the activated PP films by LTH approach based on our previous research [4].

Preparation of hydrophobic PP-TiO_2-FTCS layer

The TiO_2 coated surfaces were immersed into (5 wt%) ethanol solution of H, 1H, 2H, 2H-perfluor- dodecyl trichlorosilane (FTCS) for 48h at room temperature. Finally, the treated samples were placed in an oven at 120°C for 1h. These samples are labeled as fluorosilanizated TiO_2 coated samples (PP-TiO_2-FTCS)(see Figure1-a).

2.2.4 Fabrication of a wedge-shape track pumpless open microfluidic device

TiO_2 coated samples were patterned by using a wax template which was formed to a wedge shape with 4° wedge angle (α) and 60 mm length, for a distinct hydrophilic wedge track of limited length on a superhydrophobic surrounding, liquid flow was transported from the narrow to the wide end. 4° wedge angle (α) was the optimum wide for creating a liquid rising rivulet with its pumping ability without using pumps, valves or sorters [7b]. During the fluorosilanization of TiO_2 coated samples, only the exposed regions of the substrate were fluorosilanizated and thus only the underneath wax remained in the

hydrophilic state. Moreover, we obtained a hydrophilic path surrounded by the superhydrophobic region. Figure1-b shows the shape of a hydrophilic path and liquid flow, passing through the hydrophilic region.

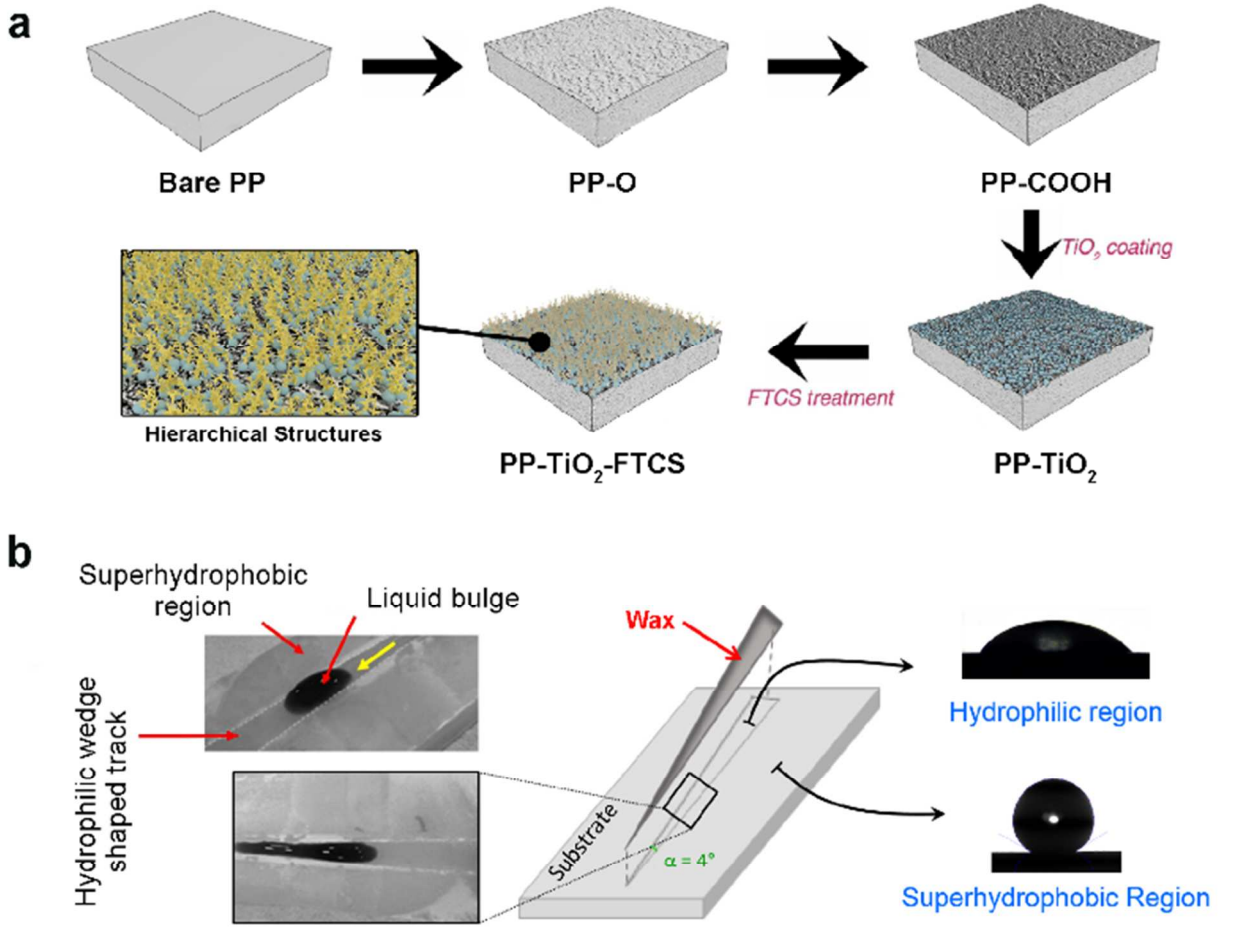

Figure 1. a) Schematic picture of hydrophilic and superhydrophobic modification process, b) Schematic representation of the methodology employed for the patterning of the surfaces, where hydrophilic regions can be imprinted onto superhydrophobic surfaces, driving of the liquid bulge and morphology of the liquid bulge.

3 Surface characterization

Wettabilities alterations were measured using Sessile drop technique by measuring the contact angles of water droplets on the flat surface of PP films. The average of five measurements by using the contact angle goniometer was reported. Also, we used Acid-base (van-Oss) approach [9] by utilizing at least three different liquids with known

parameters to calculate the surface free energy of PP films. Different properties such as chemical, mechanical, thermal and long-term stability of the wettability gradient were also examined by monitoring the contact angle changes vs. pH, temperature (°c), sonication time (min) and time (week), respectively.

The morphology and surface topography of samples was also studied by SEM-EDAX mapping (using Stereo Scan S360 Cambridge instrument) and AFM (using scanning probe microscopy, Dualscope C-26) techniques. For SEM images and EDAX analysis, samples were coated with a Cr and Carbon respectively. For AFM analysis, the samples were studied as synthesized and without any further modification. The transmission Fourier Transform Infrared Spectroscopy spectra of the samples were obtained by JASCO FT/IR-6300, Japan spectrometer. Quantitatively characterization of flow rate inside this microfluidic device was measured by using a video camera, a stopwatch, and a ruler. We used a syringe to transfer water in the hydrophilic path of the open microfluidic device. Then, the liquid movement speed was measured.

4 Biological interactions

4.1 Static and dynamic protein adsorption

To study the protein adsorption of the modified samples, Bradford assay was applied for both static and dynamic adsorption tests. For the static test, 1×1 cm^2 (0.7 gr) of each sample was immersed in 1 ml bovine serum albumin (BSA) phosphate buffer solution (PBS) (0.5 $mg.ml^{-1}$, pH 7.4) for 24 h and for the dynamic test, the samples were placed in a flow cell with constant flow of BSA solution (0.5 $mg.ml^{-1}$, pH 7.4) at 10 $ml.min^{-1}$ for 4h. Then, the supernatant was tested with Bradford method at 595 nm by using a UV-

absorbance. Then, the concentrations of protein were determined from a standard curve to measure the amounts of samples protein adsorption.

4.2 Bacterial cell attachment tests

Following the approach which was introduced in our previous publications [10], the Microtiter assay was used to determine bacterial cell attachment on the coating layer of PP film, using the two bacterial strains: *staphylococcus aureus* ATCC 25923, and *staphylococcus epidermidis* ATCC 12228. Bacterial cell attachment results were reported based on the OD and relative bacterial attachment in accordance with the following equation (Eq.1):

$$\textbf{Relative bacterial attachment}\ (\%) = \frac{\boldsymbol{OD_{Patternd\ PP\ film(Positive\ control)} - OD_{Patternd\ PP\ film\ (Negative\ control)}}}{\boldsymbol{OD_{Bare\ PP\ film(Positive\ control)} - OD_{Bare\ PP\ film\ (Negative\ control)}}} \times \mathbf{100} \quad \text{(Eq.1)}$$

In the above equation "positive control" stands for samples which are exposed to bacterial medium whereas "negative control" is for samples which are exposed to the medium but in the absence of bacteria. Based on Eq.1, the relative bacterial cell attachment for each sample is reported through calculating the difference between positive control optical density of each patterned sample and its negative control, divided by this difference for the bare sample.

4.3 Cell patterning

Murine embryonic fibroblasts, C3H/10T1/2, Clone 8 (ATCC® CCL226™) were cultured in Dulbecco's Modified Eagle's Medium (DMEM, high glucose, GlutaMAX™ Supplement, Gibco, Life Technologies Australia) containing 10% FBS (Gibco, Life Technologies Australia) and 1 % Penicillin-Streptomycin (Gibco, Life Technologies Australia) at 37°C in a humidified

atmosphere consisting of 5% CO_2. Cells at 4th passage were used for cell patterning experiment. Open microfluidic device samples were sterilized by rinsing with 70% ethanol, then with sterile PBS, followed by UV irradiation for 30 minutes. Approximately 3×10^3 cells were seeded on the sample and kept at 5% CO_2 atmosphere. 4h later, 3 ml culture media were added to the Petri dish. After 24 and 48 h, Live-Dead staining (Sigma-Aldrich, #04511-1KT-F, Castle Hill NSW, Australia) was performed according to manufacturer's protocol. Stained cells were imaged using a fluorescence microscope (Zeiss Axioskop 2).

4.4 Cell viability assay

The biocompatibility of the wettability gradients was investigated on human cervical (HeLa) and breast (MCF-7) cancer cell lines as well as non-cancerous human fibroblast cells according to International Standard Organization (ISO/EN 10993-5) protocol. Briefly, extracts of samples were prepared through the incubation of 1×1 cm^2 (0.7 gr) of each sample in 1 ml cell culture media (RPMI) following the ISO 10993-12. All the aforementioned cell lines were cultured in RPMI-1640 medium supplemented with 10% FCS and incubated in a humidified incubator at 37 °C in 5% CO_2 until 85% cell confluence was achieved. The cells were then harvested by trypsin and seeded on 96-well plates containing 200 µL medium at the density of 10^4 cells.mL^{-1} and incubated overnight under the same condition. The cultured cells were then treated with the sample extracts (20 µL per well) and incubated for different periods (24 and 48h) at the same conditions. Afterward, the medium was completely discarded and 100 µL MTT solution (0.5mg.mL^{-1} in media) was added to each well and incubated again at the same condition for 4h. The medium was then discarded again and 150 µL DMSO was added to each well to dissolve the formazan crystals and the absorbance was finally measured at 570 nm by using microplate reader. The cell viability was determined as the ratio of absorbance values

from each treatment and the control. All the experiments were repeated three times and the results were expressed as mean ± SD.

5 Result and discussion

5.1 Wettability gradient and pumpless horizontal liquid transportation

As can be seen in Table 1, bare PP sample is hydrophobic with a 99.5° water contact angle (WCA). After the TiO_2 coating, the WCA reduces to 56°, indicating its hydrophilic nature. The fluorosilanization treatment can increase the WCA to 156°, leading to a superhydrophobic surface [11].

As shown in Table 1, surface free energy measurement of PP films shows that TiO_2 layer increases surface free energy from 28.29 to 36.34 mJ/m^2, while FTCS layer can decrease it by their fluorocarbon branches to 5.51 mJ/m^2, which is in line with the water contact angle results. The increase in surface free energy (SFE) can increase surface wettability while the reduction of SFE increases the hydrophobicity of a surface.

It was reported that for rectangular track or striped surface domains, the liquid can spread and move along the long track if the WCA is smaller than a certain universal threshold value of 38°[12]. In our case, the WCA of the hydrophilic area is 56°, which is not small enough to induce pumpless transposition of water. To boost the driving force, characteristic length gradient [7b] through creating a wedge-shaped hydrophilic track was also added to the microfluidic device. In this way, Laplace pressure difference alongside wettability gradient provides enough driving force for pumpless horizontal transport of water droplet from a smaller wettable footprint (left) to a larger one (right) (see Figure1-b).

It was observed that the liquid bulge was moving on the track with the velocity of 3.2 $cm.s^{-1}$ with contact line pinned to the surface domain boundary. Another important parameter that can affect our microfluidic device performance in LOC or POC systems is liquid morphology. When liquid droplet moves on the track it can have four different morphologies of [12] a small spherical cap (i), an extended channel (ii), and drop like state with no contact (iii) or overlap (iv) with the superhydrophobic surrounding. These droplet morphologies depend on the two parameters of the track WCA and reduced volume of the liquid phase V/L^3, where V is the volume of the droplet and L is the width of the track at time "t". In our study, to avoid the first two states during droplet movement on the track with WCA of 56° and wedge angle of 4°, V was chosen large enough (V/L^3 was 12.5 at the tip while it was 3.13 at the end of the track).

Table 1. Contact angle and surface free energy values.

Sample	Bare PP	Hydrophilic PP	Superhydrophobic PP
Contact angle °	99.5	56	156
SFE γ_S (mJ/m^2)	28.29	36.34	5.51

5.2 Coating layer stability

In open pumpless microfluidics, the superhydrophobic surrounding is very important to control liquid rising stream at the micro-scale. The open microfluidic concept is usually associated with the use of free running droplets confined on hydrophilic paths enclosed by hydrophobic regions [7]. In this regard, a very high stability of this superhydrophobic surrounding is necessary that is evident in the thermal, chemical and long-term stability tests.

To evaluate the stability of the pattern; after performing experiments such as sonication, immersing in pH range solutions and temperature treatment in the oven, contact angle measurements were conducted. Long-term stability of the track was also examined in absence of UV illumination.

As can be seen in Figure2-c, superhydrophobic surrounding did not lose its superhydrophobicity (WCA> 150^{o}) when it was exposed to different pH (from 1-13) except two ends pH of one and 13, very harsh conditions. Since POC and LOC systems are not used in harsh conditions, our microfluidic device can be used in a wide range of biomedical applications. Also, it can be observed that the highest contact angle occurs at the neutral condition of pH=7. Although it was reported [13] that change in pH can varies the surface charge and could lead to a change in the conformation of FTCS molecules and subsequently contact angle and the surface wettability, in our case, the WCA variations are marginal and have an insignificant effect on the pumpless transportation of water bulge.

Ultrasonication can efficiently remove any unstable coating or surface modification as it can provide a large shear stress. Figure2-b shows that the superhydrophobic surrounding is robust and mechanically stable during the first 2 min sonication time above which the surface loses it superhydrophobicity. For POC and LOC applications, this degree of mechanical stability is acceptable. Figure2-a showed that the superhydrophobic background exhibited temperature resistance. As mentioned, one of the important drawbacks of previously reported TiO_2 based pumpless microfluidic systems was their dependence on UV illumination [4, 14]. As it shown in Figure2-d, the surface exhibited a long-term stability in the absence of UV light over the course of 28 weeks. This is related

to the dual scale roughnesses of the TiO_2 LTH deposition, which was comprehensively studied in our previous study [4].

5.3 Fourier transforms infrared spectra (FTIR)

In this study, the two different wettability regions were formed as a result of surface activation, TiO_2 nanoparticles coating followed by a fluorosilaniziation treatment where the hydrophilic and hydrophobic functional groups are usually formed. The chemical changes and successful functionalization of PP surface film can be verified by Fourier transform infrared-attenuated total reflectance (FTIR-ATR) shown in Figure2-e. As can be seen in this figure, the bare PP film and modified samples show variety characteristics of bond strength that can be attributed to different functional groups. It can be clearly seen that the PP spectrum shows strong bonds at 1600 and 1450 cm^{-1} and around 2850-2950 cm^{-1} which were assigned to the characteristic C-C and C-H vibrations, respectively. After the preparation of PP-COOH, the spectrum show characteristics of bond strength at 1710 cm^{-1} for C=O and at around 1100-1300 cm^{-1} for C-O [15]. Moreover, O-H group vibration appeared at around 3200-3400 cm^{-1} that confirmed successful covalent modifications of carboxylic groups on the surface of PP films (Figure2-e, see PP-COOH). Following PP-COOH preparation, titanium dioxide nanoparticles were coated on it. It can be clearly observed that the bonds at 760 and 680 cm^{-1} were assigned to the bending vibrations of Ti–O–Ti, and bond at 805 cm^{-1} correspond to the stretching vibrations of Ti–O [16] (Figure2-e, see PP-TiO_2). However, when TiO_2 nanoparticles were only physically deposited on the bare PP films without any treatment, no significant peaks for Ti-O or Ti-O-Ti were observed (Figure2-e, see PP/TiO_2). This proves that our surface modification was able to covalently introduce different functional groups on the "inert" PP films. Finally, after fluorosilaniziation of PP-TiO_2 (PP-TiO_2/FTCS), new characteristic

vibrational bands correspond to the stretching vibration of C-F bond can be observed at 1635, 1057, 1104 and 1106 cm^{-1}. Furthermore, the band at 1100 cm^{-1}, was assigned to Si-O stretching vibration that revealed the FTCS molecule presence (Figure2-e).

5.4 Energy dispersive X-ray analysis (EDAX)

To demonstrate the presence of FTCS and TiO_2 layer, EDAX analysis was investigated on the border of the superhydrophobic and hydrophilic regions of the microfluidic pattern. EDAX mapping results in Figure2-f2 confirmed the uniform distribution of TiO_2 nanoparticles. These results suggest that TiO_2 nanoparticles as a sublayer play a role in hydrophilic properties and provide sites for fluorosilanization of the substrate. Conversely, fluor and silane elements of FTCS molecules show a great aggregation in the superhydrophobic region of the open microfluidic device, see Figure2-f3 and f1 and Figure S1 in SI. Therefore, we can successfully exhibit that the hydrophilic track is confined by superhydrophobic surrounding with a clear border (Figure2-f1) that plays a critical role in the pumpless direction of liquids.

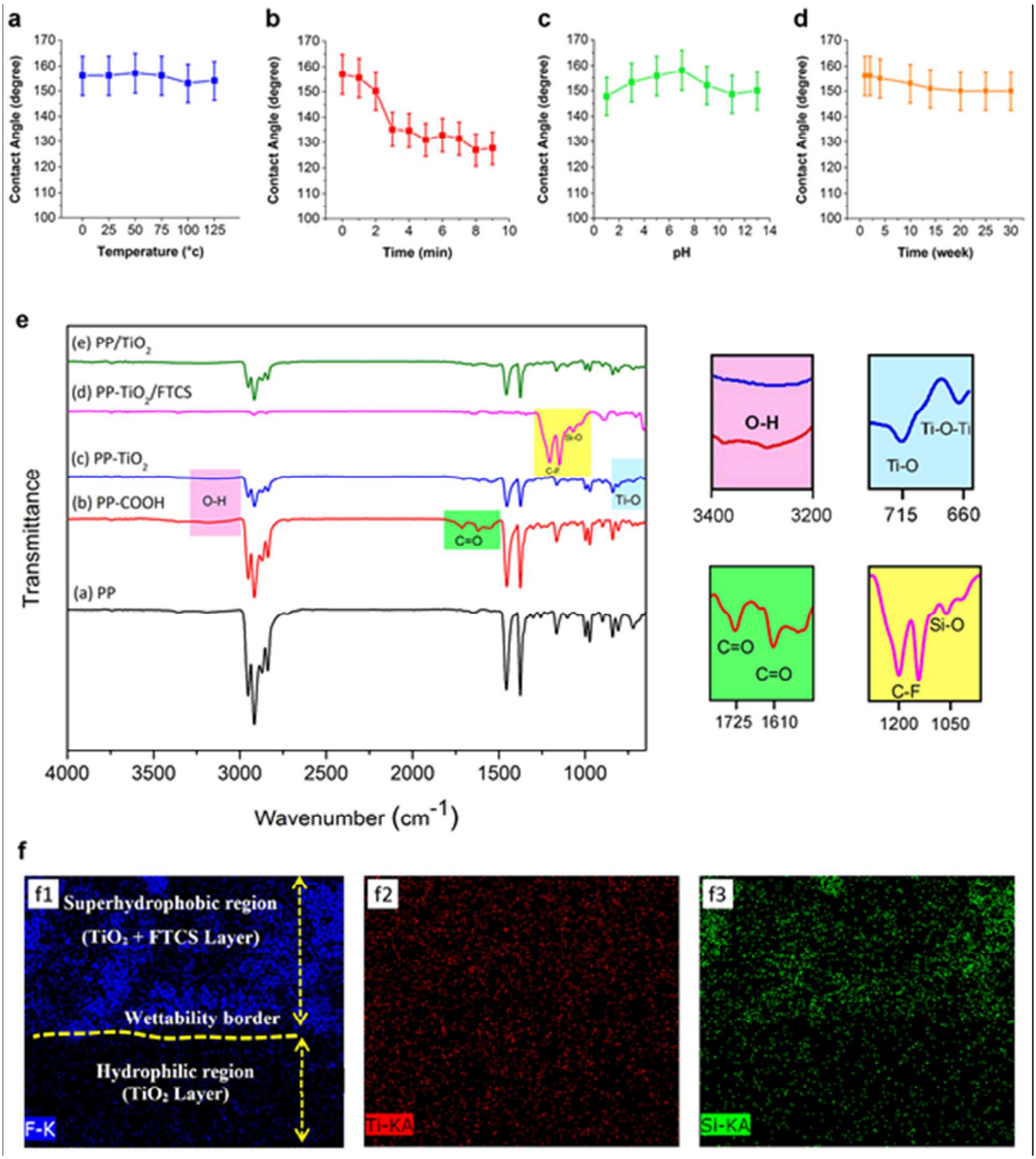

Figure 2. a) Thermal, b)mechanical, c) chemical and d) long-term stability of the superhydrophobic surrounding of the patterned PP samples. e) FTIR analysis of (a) bare PP film, (b) carboxylation of PP film, (c) covalent adsorption of a TiO_2 layer on PP film, (d) fluorosilaniziation of the PP-TiO_2 layer, and (e) non-covalent adsorption of a TiO_2 layer on pp film. f) EDAX mapping on PP-TiO_2 (f2), and of patterned PP samples (f1 and f3).

5.5 SEM and AFM analysis

The surface structure of the patterned PP film was studied by SEM and AFM techniques to show the changes in surface topography and texture. Considering the potential

biomedical applications of our microfluidic design in POC and LOC systems, the effect of the surface structure of the pattern on the interaction of biomolecules, microorganisms and cells are important and need to be considered carefully. During biosensors preparation, it is desired to increase the bioreceptor density on the sensing area to boost its system sensitivity. One way to achieve this is to increase the active surface area of the sensing regions through introducing micro-nano roughness. It is reported that often an increase in surface roughness is suitable for better cellular adhesion [17]. Rougher surfaces introduce a higher surface area and binding sites for protein adsorption and cell adhesion [17b, 18]. Also, it has reported that nano-features on a surface with intermediate wettability can introduce and promote the formation of protein aggregates and protein entering surface pores [19]. Contrary to surfaces with intermediate wettability, those with higher micron/nano scale roughness but with extreme wettability (superhydrophilicity or superhydrophobicity) behave in a different way. On a superhydrophilic surface, there is always a hydration layer, which creates a repulsive force to keep the biomolecules away from the surface [6, 20]. In the case of superhydrophobicity, the air layer on the surface dramatically reduces the interaction of biomolecules and adsorption rate [20]. Microstructural analysis of microfluidic device surface is presented in Figure3-a. The image shows two different regions of a rough superhydrophobic and smooth hydrophilic areas, which are separated by a wettability contrast border. From AFM analysis in Figure3-b, the roughness values were found 184, 81, 282 nm for bare PP film, hydrophilic track (PP-TiO_2) and superhydrophobic surrounding (PP-TiO_2-FTCS), respectively. The inset SEM image in Figure3-a revealed that the superhydrophobic surrounding has a hierarchical multilevel roughness which results in water repellency property through air

trapped and low surface energy coating layer [21]. On the other hand, SEM image of the hydrophilic surface in the microfluidic device shown in Figure S3 in SI shows nanofeature (50nm) structures comes from TiO_2 nanoparticles. The mechanism by which surface roughness alteration can change surface wettability has been well-established and discussed in the past [4, 6, 10, 14a]. According to Wenzel's model, if a surface is intrinsically hydrophilic and homogeneous (WCA<90°) any increase in roughness shifts the wettability towards superhydrophilicty but if the surface is hydrophobic (WCA>90°) that increment shifts it to superhydrophobicty. For the heterogeneous surface, a more complex model (Cassie–Baxter) is required to understand how the wettability changes when roughness varies. In Cassie–Baxter's model, water may not wet the entire surface when air pockets trapped in the surface roughness as water molecules bridge across the surface protrusions.

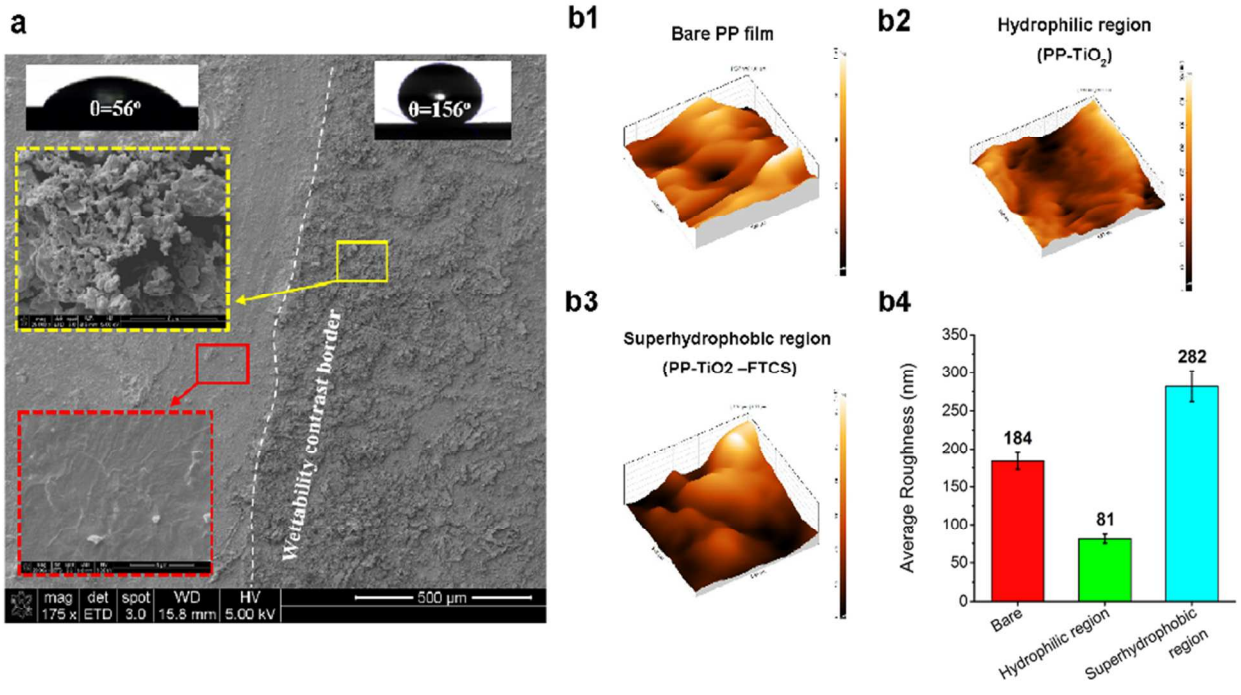

Figure 3. SEM analysis of the open microfluidic device showing the wettability contrast border (yellow-border Inset SEM image shows the hierarchical structure of the superhydrophobic area whereas the red-border inset image shows the smoother hydrophilic track, the water contact angle of each region was also identified on top

of the image), and b) AFM analysis on different regions of wedge-shaped track on 5µm by 5µm and their corresponding roughness values

6 Biological performance of the surface

6.1 Static and dynamic biomolecule adsorption

One of the important stages of POC and LOC device fabrication process is immobilization of receptors i.e. enzymes, antibodies, proteins, DNA and etc. Since the liquid is supposed to move on the hydrophilic wedge shape track, the possibility of immobilization of different biomolecules only on the track is important. BSA adsorption was studied in static and dynamic modes since it is in high density in serum and it has the ability to adhere well to surfaces [54]. When the biomolecules are going to be immobilized on the wedge shape track, the simplest way is to immerse the entire device in the biomolecules or bioreceptor solution to provide uniform immobilization of the molecules on the surface mostly through self-assembly. In this static way, it is important to only see biomolecules on the wedge-shaped track and not on the superhydrophobic surrounding.

However, when the biomolecule is going to be used as the analyte or target molecule, it is necessary to study its adsorption in a dynamic mode which is transporting the analyte solution over the track. As Figure4-b shows, the protein adsorption on the hydrophilic wedge shape track increased significantly in both static and dynamic modes, whereas a substantial reduction of protein adsorption was observed for superhydrophobic surrounding. Therefore, we can use the hydrophilic surface as a biomolecule-adhesive region and superhydrophobic substrate as non-adhesive surrounding areas. It should point out here that the hydrophilic track with this degree of protein adsorption is not suitable for the cases that liquid is going to be transported without biorecognition event. For such a

purposes, it is recommended to increase the hydrophilicity of the track toward superhydrophilicity, which is reported in our previous publication [6]. In this way, the velocity of pumpless transportation of liquid also increases as the SFE gradient increases.

From Figure4-b, it is evident that the protein adsorptions in dynamic mode are lower than that of the static mode. This is obvious as in the dynamic mode there are shear forces due to tangential flow streams that can detach the loosely attached BSA molecules from the surface. Although the micron roughness (Figure3-b) of the hydrophilic wedge-shape track is lower than that of bare PP film, its protein adsorption is significantly higher. This could be associated with the nano-roughness of the wedge shape track due to the deposition of TiO_2 nanoparticles such that average roughnesses were 52.6, 106, 187nm for bare pp, hydrophilic region (PP-TiO_2) and superhydrophobic region (PP-TiO_2-FTCS) on 1 μm by 1 μm scale, respectively (see Figure S2 and S3 in SI). There is a consensus that a surface with micron-scale roughness have a higher tendency of protein adsorption as a result of the higher surface area and porosity and more sites for protein molecules to adsorb [22].

For nano-scale roughness, two different scenarios may occur. In the first scenario, if the nano roughness results in superhydrophilicity the protein adsorption reduces because of the water barrier mechanism, that forms a physical barrier to avoid direct contact between the surface and the protein [23]. Based on molecular dynamic studies the formed hydration layer creates large repulsive forces on the proteins, which results in a lower protein adsorption [24].

In the second scenario, the nanostructured surface with intermediate wettability has the conditions which promote the formation of protein aggregates and nucleation inside the nano-pores [25]. Proteins that enter in a pore with an entrance dimension similar to their

molecules sizes, they may remain trapped and spend a longer dwelling time inside the pore. Other proteins will find a chance to enter inside the pore which causes the crowding effect and a reduction in the protein-protein distance which will be continued to the point of the formation of local supersaturation of spikes and protein nucleation and crystallization [26].

It appears that in our case, the second scenario is more effective and governs the protein adsorption phenomenon on the wedge shape track. As expected, the superhydrophobic surrounding exhibited a substantial reduction in BSA adsorption due to air packets trapped underneath of the BSA solution, which significantly reduces the surface accessibility and active adsorption sites [10].

As can be observed from Figure4-c, on the hydrophilic wedge shape track with WCA of 56°, the relative bacterial attachment is about 41% and 56% for *staphylococcus aureus* and *staphylococcus epidermidis*, respectively. These values even reduced to 16.66 and 22 for superhydrophobic surrounding. These results evidence that microbes are more prone to migrate to the hydrophilic wedge shape track than its background, which makes our microfluidic device a very attractive candidate for whole-cell biosensors which are a good alternative to enzyme-based biosensors [27]. It should point out here that bacterial adhesion on superhydrophobic surfaces is very dependent on the type of microorganism, surface topography and texture and surface composition. These variations make the mechanism of biological adhesion on superhydrophobic surfaces very difficult to clarify and have led to many inconsistent reports. It is known that superhydrophobic surface can inhibit microbial adhesion due to their very good repellency. However, there are several reports that have also suggested superhydrophobic surfaces not only cannot reduce bacterial attachment but also induce more adhesion [28]. Therefore,

superhydrophobic surrounding for pumpless microfluidic systems for whole-cell biosensors should be strategically designed to not have hydrophobic-hydrophobic interaction between background and the selected microorganism.

6.2 Spatial control of cell adhesion

Cellular patterning on artificial substrates is a necessary component to the study of fundamental cell biology, as well as biomedical engineering such as cell-based biosensors [29], cell culture analogs [30], tissue engineering [31] and microfluidic assays [29b, 32]. Patterning of cells [29b, 32a, 33], proteins [34] and other biomolecules [35] onto a substrate without the need for drying can be applied by microfluidic devices. Microfluidics can produce highly accurate parallel patterns of many different molecules, which is not possible with other patterning methods [35a, 35b]. To demonstrate the cell patterning on the open microfluidic device, cell attachment and growth were studied. Different parts of TiO_2 coated sample were examined to see the attachment of murine embryonic fibroblasts. Fluorescence microscopy analysis showed a good cellular attachment after LTH TiO_2 coating (Figure S4). Figure4-a and Figure S5 in SI show fluorescence images of patterned murine embryonic fibroblasts on the wedge-shaped track after 24h culture. Cells preferentially attached and spread on hydrophilic region. This indicates the ability to design and create patterned structures in an open microfluidic device. After 2 days of growth, cells selectively spread, proliferate and form a confluent layer on the hydrophilic track of the microfluidic device (Figure S5-f) whilst superhydrophobic surrounding inhibited cell attachment and growth. It was found out that the prevention of intimate contact of the surface with biological fluid by altering physicochemical properties of the surface creates an anti-adhesion characteristic that reduces the attachment of biological agents like proteins and cells. The water repellency of superhydrophobic surface causes the prevention of contact between the culture medium and cells with entire surface. Cell adhesion can be applied through the extracellular matrix (ECM)

mediating proteins that pre-absorbed and interacted with the surface. These facts suggest that the reduction in protein adsorption can limit cellular adhesion onto the surface [22, 36]. Cellular adhesion study on surface revealed that the wettability of artificial materials plays a critical role in cell adhesion. Tamada et al [37] claimed that cells effectively adhere onto polymer surfaces with a water contact angle of 70°. Also, the other study indicated that surface with water contact angles of 40–70° presenting moderate wettability and give the most suitable surface for cell adhesion [37-38]. Surface properties such as chemistry, wettability, charge, roughness and material stiffness can affect the ability of cells to adhere. Patterning these properties allows for spatial control over cell attachment. Wettability is often considered a dominant parameter as it directly affects the conformation of mediating proteins on the surface. The differences in protein conformation on hydrophobic and hydrophilic surfaces have been directly linked to increased cell spreading and adhesion on hydrophilic surfaces [39]. Because, serum proteins adsorb to the surface, prior to the cell attachment and subsequent cells binding. Therefore, for the spatial control of cell adhesion, we created hydrophilic regions which are surrounded by the hydrophobic areas.

6.3 Cell viability assay

Regarding the significant effects of the surface chemistry and topography on the cell viability, a comprehensive study was conducted in order to clarify the probable adverse effects of the surface modification of PP samples on the cell viability. Different results obtained by MTT assay depending on the sample, exposure time and cell line (Figure4-d). Overall results indicate a negligible cell toxicity of engineered samples. The minimum cell viability of 90.85% obtained after 48 h incubation of MCF-7 cells with 20 μL hydrophilic sample extract. Interestingly, the cell viability of 97.92 and 98.15% obtained at the same condition for fibroblast and HeLa cells, respectively, indicating the cell line dependent effects of the surface engineering. Among the

tested samples, the superhydrophobic sample was found more biocompatible (see Figure4-d). Moreover, MCF-7 cells seem more sensitive to the surface engineering of the sample than fibroblast and HeLa cells. According to these results, no significant cytotoxicity occurred following the surface modification of the samples. Microscopic monitoring of cells after 48h exposure to hydrophilic sample extract revealed no significant change in MCF-7, HeLa and fibroblast cells morphology (Figure S6 in SI), indicating normal growth of the cells. So with the cells displaying their normal morphology, we can introduce the safe substrate for cell patterning in microfluidic devices.

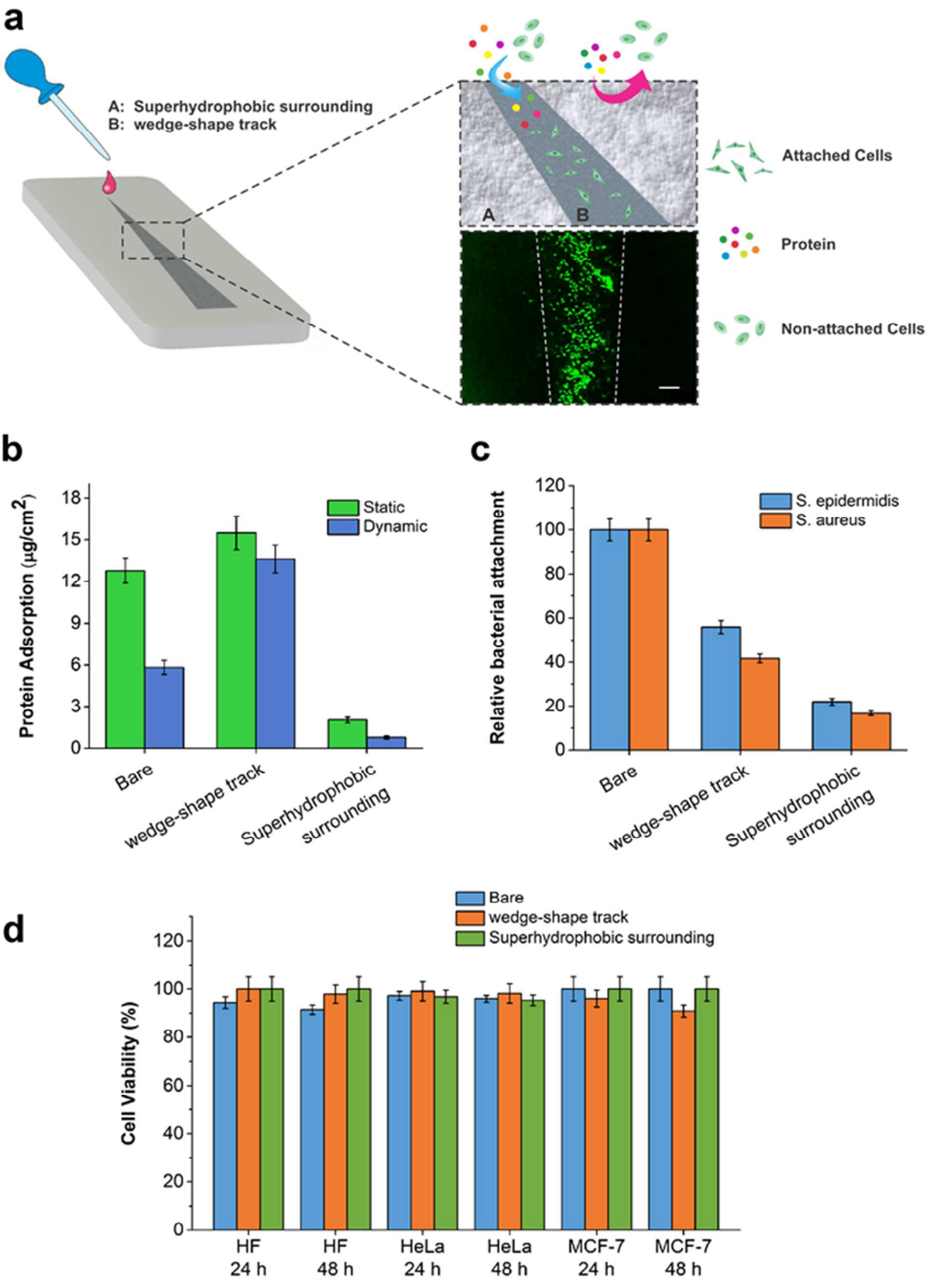
a
A: Superhydrophobic surrounding
B: wedge-shape track
A
B
Attached Cells
Protein
Non-attached Cells
b
Protein Adsorption (μg/cm²)
Static
Dynamic
Bare
wedge-shape track
Superhydrophobic surrounding
c
Relative bacterial attachment
S. epidermidis
S. aureus
Bare
wedge-shape track
Superhydrophobic surrounding
d
Bare
wedge-shape track
Superhydrophobic surrounding
Cell Viability (%)
HF 24 h
HF 48 h
HeLa 24 h
HeLa 48 h
MCF-7 24 h
MCF-7 48 h

Figure 4. a) Fluorescence micrograph of murine embryonic fibroblasts cultured on PP patterned substrates. Spreading and proliferation of patterned cells into a confluent layer was achieved, b) Static and dynamic BSA protein adsorption capacity of PP samples, c) Relative bacterial cell attachment for different PP samples using microtiter assay, d) Viability percentage of non-cancerous humane fibroblast (HF), HeLa and MCF-7 cells after 24 and 48 hour exposure with PP samples.

6.4 Antibody sensing

One of the main objectives of this study is to show the applicability of our device as a biosensor for the detection of an analyte through a recognition with a bio-receptor attached on the hydrophilic track surface, for example, by means of an immunoassay. For the proof-of-principle of biosensing application, we employed the well-known high-affinity molecular couple of BSA-antiBSA as a biological model. The biofunctionalization of the hydrophilic track of the device by BSA antigen probes as receptors can be performed through physisorption (physical adsorption) and chemical covalent attachment using salinization chemistry. For the covalent attachment of BSA bioreceptors, Isocyanatopropyltriethoxysilane (ICPTS) was used because of its ability to anchor directly to amino groups of BSA, thus avoiding the use of crosslinkers. The silane agent is coupled to the –OH groups of the TiO_2 coated hydrophilic track of the device while the BSA molecules are attached to the isocyanate moieties of ICPTS. This was performed by simply immersing the chip in a solution of 2% of ICPTS in toluene/ethanol under N_2 atmosphere for 1 hr. Then, the device with hydrophilic track coated by ICPTS organosilane was soaked in BSA solution with different concentrations for 2 hrs to find the optimum concentration of BSA to functionalize the track. As shown in Figure S7a, the optimum concentration of BSA was found 3 µg/ml. In order to test the biosensing efficiency of the BSA-functionalized microfluidic device, droplets (50 µl) of Cy5-labelled antiBSA with different concentrations (0.5, 1, 2, 4, 6 and 8 µg/ml) were dispensed over the tip of the track and incubated for 15 minutes.

After rinsing and drying, the fluorescence of the Cy5 was examined in order to characterize the binding efficiency of the antiBSA with the BSA probes previously attached to the hydrophilic track surface. As can be seen in Figure S7b, the sensitivity of the device was found 1 µg/ml of analyte concentration below which the fluorescence cannot be observed. For physically absorbed BSA antigen probes on the track, the detection limit increased significantly to 4 µg/ml, as expected. This proof-of-concept result shows the great potential of this device in biosensing and diagnostics mainly due to the functionality of the hydrophilic TiO_2 coated track which provides a platform to immobilize a variety of bioreceptors.

7 Strategies for designing pumpless microfluidic devices:

In a design of pumpless LOC or POC systems, important considerations should be taken into account as listed below:

- The hydrophilicity of the confined track should be adjusted based on its defined role; if the track is going to be used as only the channel for transporting liquid from one point to another part of the chip, superhydrophlicity is preferred. However, if any biorecognition event is going to occur on the track, intermediate wettability is desired (40^o < WCA < 70^o)[40]. It should point out here that if the track does not have characteristic length gradient e.g. rectangular shape, for the liquid to spread on the track WCA must be below the threshold value of 38^o[12]. This may compromise the cellular or biomolecular adsorption capacity of the track.
- In order to generate enough SFE gradient, the hydrophobicity of the track background or surrounding area should be the highest possible value. It should be noted that if the microfluidic pumpless device is going to be used as the cell-based biosensor, a careful selection of superhydrophobic routes, surface energy reducer chemicals, and roughness is critical to have cells patterned or immobilized only on the hydrophilic track. The velocity

of liquid transportation can be adjusted by simply changing the degree of background hydrophobicity.

- Track geometry and shape is also important parameter on the performance of such a pumpless microfluidic systems. Surface free energy gradient with low contact angle hysteresis ($10^{o} \leq$) [41] is required to let water droplet move freely. The gradient of characteristic length (such as a wedge-shaped track) can also induce Laplace pressure difference on the asymmetric droplet. Wedge angles of up to 5^{o} are suggested to have the maximum driving capillary force without the compromise of the diminishing of the travel distance [7b].
- Pre-wetting (presuffusing) of the hydrophilic track can increase the liquid transport speed by submerging the crevices of the track.
- Track roughness, topography, and texture can affect protein adsorption and the biological processes of cells. The effects of track roughness are cell-type dependent because cells will respond best to surfaces which mimic their physiological environment. Generally, a higher surface roughness provides a higher availability of protein binding sites and better cellular adhesion. However, an increase in track roughness can shift the track wettability toward superhydrophlicty and reduction in protein and cellular adhesion. While creating ridges or groves on the track can direct cells orientations, sharp features or edges on the track can avoid cell proliferation and may lead to cellular rejection [42].

Conclusion

In this paper, a stable and biocompatible wedge-shape hydrophilic track which was confined by a superhydrophobic surrounding was fabricated on "inert" PP films to transport biological fluids without the need for a pump or any input energy. It was exhibited that the degree of hydrophilicity of the track needs to be carefully adjusted for any biosensing applications. The

designed microfluidic device with intermediate wettability showed that it has a superior potential to be used as the platform for protein-based biosensors. In dynamic mode, BSA adsorption increased from 5.83 on bare PP film to 13.61 μg/cm^2 on the track while almost no protein adsorption was observed on the superhydrophobic surrounding. For bacterial based biosensing, the hydrophilic track showed bacterial attachment. However, the superhydropbioc surrounding also exhibited a low degree of bacterial attachment for staphylococcus aureus and staphylococcus epidermidis. The patterns also showed a good cell patterning ability such that murine embryonic fibroblasts were interestingly only attached and aligned along the wedge shape hydrophilic track. This suggests that the device can be considered as a suitable candidate for fundamental cell biology. In general, the results of this study revealed that the introduced LTH surface engineering approach using TiO_2 nanoparticles have a great potential to be used for the commercial implementation of pumpless transportation of biological fluids on an inert plastic substrate (Lab-on-Plastic) for point-of-care applications.

References

1. (a) Mertaniemi, H.; Jokinen, V.; Sainiemi, L.; Franssila, S.; Marmur, A.; Ikkala, O.; Ras, R. H., Superhydrophobic Tracks for Low-Friction, Guided Transport of Water Droplets. *Advanced Materials* **2011,** *23* (26), 2911-2914; (b) Balu, B.; Berry, A. D.; Hess, D. W.; Breedveld, V., Patterning of superhydrophobic paper to control the mobility of micro-liter drops for two-dimensional lab-on-paper applications. *Lab on a Chip* **2009,** *9* (21), 3066-3075; (c) You, I.; Kang, S. M.; Lee, S.; Cho, Y. O.; Kim, J. B.; Lee, S. B.; Nam, Y. S.; Lee, H., Polydopamine Microfluidic System toward a Two-Dimensional, Gravity-Driven Mixing Device. *Angewandte Chemie International Edition* **2012,** *51* (25), 6126-6130; (d) Sousa, M. P.; Mano, J. o. F., Superhydrophobic paper in the development of disposable labware and lab-on-paper devices. *ACS applied materials & interfaces* **2013,** *5* (9), 3731-3737; (e) Elsharkawy, M.; Schutzius, T. M.; Megaridis, C. M., Inkjet patterned superhydrophobic paper for open-air surface microfluidic devices. *Lab on a Chip* **2014,** *14* (6), 1168-1175; (f) Zhao, Y.; Xu, Z.; Niu, H.; Wang, X.; Lin, T., Magnetic liquid marbles: Toward "lab in a droplet". *Advanced Functional Materials* **2015,** *25* (3), 437-444; (g) Kim, D.; Seo, J.; Shin, S.; Lee, S.; Lee, K.; Cho, H.; Shim, W.; Lee, H.-B.-R.; Lee, T., Reversible liquid adhesion switching of superamphiphobic Pd-decorated Ag dendrites via gas-induced structural changes. *Chemistry of Materials* **2015,** *27* (14), 4964-4971; (h) Jönsson-Niedziółka, M.; Lapierre, F.; Coffinier, Y.; Parry, S.;

Zoueshtiagh, F.; Foat, T.; Thomy, V.; Boukherroub, R., EWOD driven cleaning of bioparticles on hydrophobic and superhydrophobic surfaces. *Lab on a Chip* **2011,** *11* (3), 490-496; (i) Lapierre, F.; Piret, G.; Drobecq, H.; Melnyk, O.; Coffinier, Y.; Thomy, V.; Boukherroub, R., High sensitive matrix-free mass spectrometry analysis of peptides using silicon nanowires-based digital microfluidic device. *Lab on a Chip* **2011,** *11* (9), 1620-1628; (j) Lapierre, F.; Harnois, M.; Coffinier, Y.; Boukherroub, R.; Thomy, V., Split and flow: reconfigurable capillary connection for digital microfluidic devices. *Lab on a Chip* **2014,** *14* (18), 3589-3593; (k) Li, L.; Breedveld, V.; Hess, D. W., Hysteresis controlled water droplet splitting on superhydrophobic paper. *Colloid and Polymer Science* **2013,** *291* (2), 417-426.

2. Li, X.; Ballerini, D. R.; Shen, W., A perspective on paper-based microfluidics: current status and future trends. *Biomicrofluidics* **2012,** *6* (1), 011301.

3. Zhou, M.; Li, J.; Zhang, M.; Wang, H.; Lan, Y.; Wu, Y.-n.; Li, F.; Li, G., A polydopamine layer as the nucleation center of MOF deposition on "inert" polymer surfaces to fabricate hierarchically structured porous films. *Chem. Commun.* **2015,** *51* (13), 2706-2709.

4. Razmjou, A.; Mansouri, J.; Chen, V.; Lim, M.; Amal, R., Titania nanocomposite polyethersulfone ultrafiltration membranes fabricated using a low temperature hydrothermal coating process. *J. Membr. Sci.* **2011,** *380* (1–2), 98-113.

5. Razmjou, A.; Arifin, E.; Dong, G.; Mansouri, J.; Chen, V., Superhydrophobic modification of TiO2 nanocomposite PVDF membranes for applications in membrane distillation. *J. Membr. Sci.* **2012,** *415–416*, 850-863.

6. Noorisafa, F.; Razmjou, A.; Emami, N.; Low, Z.-X.; Korayem, A. H.; Kajani, A. A., Surface modification of polyurethane via creating a biocompatible superhydrophilic nanostructured layer: role of surface chemistry and structure. *Journal of Experimental Nanoscience* **2016,** *11* (14), 1087-1109.

7. (a) Huang, S.; Song, J.; Lu, Y.; Chen, F.; Zheng, H.; Yang, X.; Liu, X.; Sun, J.; Carmalt, C. J.; Parkin, I. P., Underwater Spontaneous Pumpless Transportation of Nonpolar Organic Liquids on Extreme Wettability Patterns. *ACS applied materials & interfaces* **2016,** *8* (5), 2942-2949; (b) Ghosh, A.; Ganguly, R.; Schutzius, T. M.; Megaridis, C. M., Wettability patterning for high-rate, pumpless fluid transport on open, non-planar microfluidic platforms. *Lab on a Chip* **2014,** *14* (9), 1538-1550.

8. Lee, K. W.; McCarthy, T. J., Surface-selective hydroxylation of polypropylene. *Macromolecules* **1988,** *21* (2), 309-313.

9. Van Oss, C.; Ju, L.; Chaudhury, M.; Good, R., Estimation of the polar parameters of the surface tension of liquids by contact angle measurements on gels. *Journal of Colloid and Interface Science* **1989,** *128* (2), 313-319.

10. Moazzam, P.; Razmjou, A.; Golabi, M.; Shokri, D.; Landarani-Isfahani, A., Investigating the BSA protein adsorption and bacterial adhesion of Al-alloy surfaces after creating a hierarchical (micro/nano) superhydrophobic structure. *Journal of Biomedical Materials Research Part A* **2016**.

11. K Webb, H.; Hasan, J.; K Truong, V.; J Crawford, R.; P Ivanova, E., Nature inspired structured surfaces for biomedical applications. *Current medicinal chemistry* **2011,** *18* (22), 3367-3375.

12. Brinkmann, M.; Lipowsky, R., Wetting morphologies on substrates with striped surface domains. *Journal of applied physics* **2002,** *92* (8), 4296-4306.

13. (a) Peng, S.; Yang, X.; Tian, D.; Deng, W., Chemically stable and mechanically durable superamphiphobic aluminum surface with a micro/nanoscale binary structure. *ACS applied materials & interfaces* **2014,** *6* (17), 15188-15197; (b) Zhu, S.; Li, Y.; Zhang, J.; Lü, C.; Dai, X.; Jia, F.; Gao, H.; Yang, B., Biomimetic polyimide nanotube arrays with slippery or sticky superhydrophobicity. *Journal of colloid and interface science* **2010,** *344* (2), 541-546.

14. (a) Razmjou Chaharmahali, A. The effect of TiO2 nanoparticles on the surface chemistry, structure and fouling performance of polymeric membranes. University of New South Wales. Chemical Sciences & Engineering, Sydney Australia, 2012; (b) Caputo, G.; Cortese, B.; Nobile, C.; Salerno, M.; Cingolani, R.; Gigli, G.; Cozzoli, P. D.; Athanassiou, A., Reversibly Light-Switchable Wettability of Hybrid

Organic/Inorganic Surfaces With Dual Micro-/Nanoscale Roughness. *Advanced Functional Materials* **2009,** *19* (8), 1149-1157.

15. (a) Nakason, C.; Wannavilai, P.; Kaesaman, A., Thermoplastic vulcanizates based on epoxidized natural rubber/polypropylene blends: effect of compatibilizers and reactive blending. *Journal of applied polymer science* **2006,** *100* (6), 4729-4740; (b) Nakason, C.; Saiwari, S.; Kaesaman, A., Rheological properties of maleated natural rubber/polypropylene blends with phenolic modified polypropylene and polypropylene-g-maleic anhydride compatibilizers. *Polymer testing* **2006,** *25* (3), 413-423.

16. (a) Zeitler, V. A.; Brown, C. A., The infrared spectra of some Ti-O-Si, Ti-O-Ti and Si-O-Si compounds. *The Journal of Physical Chemistry* **1957,** *61* (9), 1174-1177; (b) Vasconcelos, D. C. L.; Nunes, E. H. M.; Gasparon, M.; Vasconcelos, W. L., Infrared spectroscopy of titania sol-gel coatings on 316L stainless steel. *Materials sciences and applications* **2011,** *2* (10), 1375.

17. (a) Bowers, K. T.; Keller, J. C.; Randolph, B. A.; Wick, D. G.; Michaels, C. M., Optimization of surface micromorphology for enhanced osteoblast responses in vitro. *International Journal of Oral & Maxillofacial Implants* **1992,** *7* (3); (b) Lampin, M.; Warocquier-Clérout, R.; Legris, C.; Degrange, M.; Sigot-Luizard, M., Correlation between substratum roughness and wettability, cell adhesion, and cell migration. *Journal of biomedical materials research* **1997,** *36* (1), 99-108; (c) Deligianni, D. D.; Katsala, N. D.; Koutsoukos, P. G.; Missirlis, Y. F., Effect of surface roughness of hydroxyapatite on human bone marrow cell adhesion, proliferation, differentiation and detachment strength. *Biomaterials* **2000,** *22* (1), 87-96; (d) Huang, H.-H.; Ho, C.-T.; Lee, T.-H.; Lee, T.-L.; Liao, K.-K.; Chen, F.-L., Effect of surface roughness of ground titanium on initial cell adhesion. *Biomolecular engineering* **2004,** *21* (3), 93-97.

18. Martínez, E. C.; Hernández, J. C. R.; Machado, M.; Mano, J. F.; Ribelles, J. L. G.; Pradas, M. M.; Sánchez, M. S., Human chondrocyte morphology, its dedifferentiation, and fibronectin conformation on different PLLA microtopographies. *Tissue Engineering Part A* **2008,** *14* (10), 1751-1762.

19. Benesch, T.; Yiacoumi, S.; Tsouris, C., Brownian motion in confinement. *Physical Review E* **2003,** *68* (2), 021401.

20. Orooji, Y.; Faghih, M.; Razmjou, A.; Hou, J.; Moazzam, P.; Emami, N.; Aghababaie, M.; Nourisfa, F.; Chen, V.; Jin, W., Nanostructured mesoporous carbon polyethersulfone composite ultrafiltration membrane with significantly low protein adsorption and bacterial adhesion. *Carbon* **2017,** *111*, 689-704.

21. (a) Marmur, A., The lotus effect: superhydrophobicity and metastability. *Langmuir* **2004,** *20* (9), 3517-3519; (b) Cassie, A., Contact angles. *Discussions of the Faraday Society* **1948,** *3*, 11-16; (c) Wang, S.; Jiang, L., Definition of superhydrophobic states. *Advanced Materials* **2007,** *19* (21), 3423-3424.

22. Song, W.; Mano, J. F., Interactions between cells or proteins and surfaces exhibiting extreme wettabilities. *Soft Matter* **2013,** *9* (11), 2985-2999.

23. (a) Zheng, J.; Li, L.; Chen, S.; Jiang, S., Molecular simulation study of water interactions with oligo (ethylene glycol)-terminated alkanethiol self-assembled monolayers. *Langmuir* **2004,** *20* (20), 8931-8938; (b) Pertsin, A. J.; Grunze, M., Computer simulation of water near the surface of oligo (ethylene glycol)-terminated alkanethiol self-assembled monolayers. *Langmuir* **2000,** *16* (23), 8829-8841; (c) Archambault, J. G.; Brash, J. L., Protein repellent polyurethane-urea surfaces by chemical grafting of hydroxyl-terminated poly (ethylene oxide): effects of protein size and charge. *Colloids and Surfaces B: Biointerfaces* **2004,** *33* (2), 111-120; (d) Hou, J.; Dong, G.; Ye, Y.; Chen, V., Enzymatic degradation of bisphenol-A with immobilized laccase on TiO2 sol–gel coated PVDF membrane. *Journal of Membrane Science* **2014,** *469*, 19-30.

24. Zheng, J.; Li, L.; Tsao, H.-K.; Sheng, Y.-J.; Chen, S.; Jiang, S., Strong repulsive forces between protein and oligo (ethylene glycol) self-assembled monolayers: A molecular simulation study. *Biophysical journal* **2005,** *89* (1), 158-166.

25. Scopelliti, P. E.; Borgonovo, A.; Indrieri, M.; Giorgetti, L.; Bongiorno, G.; Carbone, R.; Podestà, A.; Milani, P., The Effect of Surface Nanometre-Scale Morphology on Protein Adsorption. *PLoS ONE* **2010,** *5* (7), e11862.

26. Chayen, N. E.; Saridakis, E.; Sear, R. P., Experiment and theory for heterogeneous nucleation of protein crystals in a porous medium. *Proceedings of the National Academy of Sciences of the United States of America* **2006,** *103* (3), 597-601.
27. Park, M.; Tsai, S.-L.; Chen, W., Microbial Biosensors: Engineered Microorganisms as the Sensing Machinery. *Sensors* **2013,** *13* (5), 5777.
28. Zhu, H.; Guo, Z.; Liu, W., Adhesion behaviors on superhydrophobic surfaces. *Chem. Commun.* **2014,** *50* (30), 3900-3913.
29. (a) Park, T. H.; Shuler, M. L., Integration of cell culture and microfabrication technology. *Biotechnology progress* **2003,** *19* (2), 243-253; (b) Chiu, D. T.; Jeon, N. L.; Huang, S.; Kane, R. S.; Wargo, C. J.; Choi, I. S.; Ingber, D. E.; Whitesides, G. M., Patterned deposition of cells and proteins onto surfaces by using three-dimensional microfluidic systems. *Proceedings of the National Academy of Sciences* **2000,** *97* (6), 2408-2413.
30. (a) Sweeney, L.; Shuler, M.; Babish, J.; Ghanem, A., A cell culture analogue of rodent physiology: Application to naphthalene toxicology. *Toxicology in vitro* **1995,** *9* (3), 307-316; (b) Shuler, M.; Ghanem, A.; Quick, D.; Wong, M.; Miller, P., A self-regulating cell culture analog device to mimic animal and human toxicological responses. *Biotechnology and bioengineering* **1996,** *52* (1), 45-60.
31. Yang, J.; Yamato, M.; Kohno, C.; Nishimoto, A.; Sekine, H.; Fukai, F.; Okano, T., Cell sheet engineering: recreating tissues without biodegradable scaffolds. *Biomaterials* **2005,** *26* (33), 6415-6422.
32. (a) Tan, W.; Desai, T. A., Microfluidic patterning of cells in extracellular matrix biopolymers: effects of channel size, cell type, and matrix composition on pattern integrity. *Tissue engineering* **2003,** *9* (2), 255-267; (b) Rhee, S. W.; Taylor, A. M.; Tu, C. H.; Cribbs, D. H.; Cotman, C. W.; Jeon, N. L., Patterned cell culture inside microfluidic devices. *Lab on a Chip* **2005,** *5* (1), 102-107.
33. Folch, A.; Ayon, A.; Hurtado, O.; Schmidt, M.; Toner, M., Molding of deep polydimethylsiloxane microstructures for microfluidics and biological applications. *Journal of Biomechanical Engineering* **1999,** *121* (1), 28-34.
34. (a) Folch, A.; Toner, M., Cellular micropatterns on biocompatible materials. *Biotechnology progress* **1998,** *14* (3), 388-392; (b) De Silva, M. N.; Desai, R.; Odde, D. J., Micro-patterning of animal cells on PDMS substrates in the presence of serum without use of adhesion inhibitors. *Biomedical microdevices* **2004,** *6* (3), 219-222.
35. (a) Delamarche, E.; Bernard, A.; Schmid, H.; Michel, B.; Biebuyck, H., Patterned delivery of immunoglobulins to surfaces using microfluidic networks. *Science* **1997,** *276* (5313), 779-781; (b) Delamarche, E.; Bernard, A.; Schmid, H.; Bietsch, A.; Michel, B.; Biebuyck, H., Microfluidic networks for chemical patterning of substrates: design and application to bioassays. *Journal of the American Chemical Society* **1998,** *120* (3), 500-508; (c) Patel, N.; Padera, R.; Sanders, G. H.; Cannizzaro, S. M.; Davies, M. C.; Langer, R.; Roberts, C. J.; Tendler, S. J.; Williams, P. M.; Shakesheff, K. M., Spatially controlled cell engineering on biodegradable polymer surfaces. *The FASEB journal* **1998,** *12* (14), 1447-1454.
36. Koc, Y.; De Mello, A.; McHale, G.; Newton, M.; Roach, P.; Shirtcliffe, N., Nano-scale superhydrophobicity: suppression of protein adsorption and promotion of flow-induced detachment. *Lab on a Chip* **2008,** *8* (4), 582-586.
37. Tamada, Y.; Ikada, Y., Effect of preadsorbed proteins on cell adhesion to polymer surfaces. *Journal of colloid and interface science* **1993,** *155* (2), 334-339.
38. (a) Lee, J. H.; Lee, J. W.; Khang, G.; Lee, H. B., Interaction of cells on chargeable functional group gradient surfaces. *Biomaterials* **1997,** *18* (4), 351-358; (b) Van Wachem, P.; Beugeling, T.; Feijen, J.; Bantjes, A.; Detmers, J.; Van Aken, W., Interaction of cultured human endothelial cells with polymeric surfaces of different wettabilities. *Biomaterials* **1985,** *6* (6), 403-408; (c) Tamada, Y.; Ikada, Y., Cell adhesion to plasma-treated polymer surfaces. *Polymer* **1993,** *34* (10), 2208-2212; (d) Lee, J. H.; Khang, G.; Lee, J. W.; Lee, H. B., Interaction of different types of cells on polymer surfaces with wettability gradient. *Journal of colloid and interface science* **1998,** *205* (2), 323-330; (e) Van Wachem, P.; Hogt, A.;

Beugeling, T.; Feijen, J.; Bantjes, A.; Detmers, J.; Van Aken, W., Adhesion of cultured human endothelial cells onto methacrylate polymers with varying surface wettability and charge. *Biomaterials* **1987,** *8* (5), 323-328; (f) Tamada, Y.; Ikada, Y., Cell attachment to various polymer surfaces. In *Polymers in medicine II*, Springer: 1986; pp 101-115.

39. (a) Barrias, C. C.; Martins, M. C. L.; Almeida-Porada, G.; Barbosa, M. A.; Granja, P. L., The correlation between the adsorption of adhesive proteins and cell behaviour on hydroxyl-methyl mixed self-assembled monolayers. *Biomaterials* **2009,** *30* (3), 307-316; (b) García, A. J.; Vega, M. a. D.; Boettiger, D., Modulation of cell proliferation and differentiation through substrate-dependent changes in fibronectin conformation. *Molecular biology of the cell* **1999,** *10* (3), 785-798.

40. Arima, Y.; Iwata, H., Effect of wettability and surface functional groups on protein adsorption and cell adhesion using well-defined mixed self-assembled monolayers. *Biomaterials* **2007,** *28* (20), 3074-3082.

41. Chaudhury, M. K.; Whitesides, G. M., How to Make Water Run Uphill. *Science* **1992,** *256* (5063), 1539-1541.

42. Dechene, J. M. Surface Modifications of Poly (dimethylsiloxane) for Biological Application of Microfluidic Devices. The University of Western Ontario, 2010.